Stem Cell Research 81 (2024) 103583

Contents lists available at ScienceDirect

Stem Cell Research

journal homepage: www.elsevier.com/locate/scr

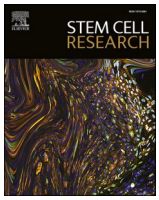

Ice recrystallization inhibitors enable efficient cryopreservation of induced pluripotent stem cells: A functional and transcriptomic analysis

Kathleen Mommaerts [a,b,*], Satoshi Okawa [b,1], Margaux Schmitt [a], Olga Kofanova [a], Tracey R. Turner [c], Robert N. Ben [c,d], Antonio Del Sol [b,e,f], William Mathieson [a], Jens C. Schwamborn [b], Jason P. Acker [c,g], Fay Betsou [a,2]

[a] Integrated Biobank of Luxembourg, Luxembourg Institute of Health, 1 rue Louis Rech, L-3555 Dudelange, Luxembourg
[b] Luxembourg Centre for Systems Biomedicine (LCSB), University of Luxembourg, 2 avenue de Université, L-4365 Esch-sur-Alzette, Luxembourg
[c] PanTHERA CryoSolutions Inc., Edmonton, Alberta, Canada
[d] Department of Chemistry, University of Ottawa, Ottawa, Ontario, Canada
[e] CIC bioGUNE, Bizkaia Technology Park, 48160 Derio, Spain
[f] IKERBASQUE, Basque Foundation for Science, Bilbao 48013, Spain
[g] Laboratory Medicine and Pathology, University of Alberta, Edmonton, Alberta, Canada

ARTICLE INFO

Keywords:
Ice recrystallization inhibitors
Induced pluripotent stem cells
Cryopreservation
Transcriptome
DMSO
Pluripotency
CryoStor®
iPSCs

ABSTRACT

The successful use of human induced pluripotent stem cells (iPSCs) for research or clinical applications requires the development of robust, efficient, and reproducible cryopreservation protocols. After cryopreservation, the survival rate of iPSCs is suboptimal and cell line-dependent. We assessed the use of ice recrystallization inhibitors (IRIs) for cryopreservation of human iPSCs. A toxicity screening study was performed to assess specific small-molecule carbohydrate-based IRIs and concentrations for further evaluation. Then, a cryopreservation study compared the cryoprotective efficiency of 15 mM IRIs in 5 % or 10 % DMSO-containing solutions and with CryoStor® CS10. Three iPSC lines were cryopreserved as single-cell suspensions in the cryopreservation solutions and post-thaw characteristics, including pluripotency and differential gene expression were assessed. We demonstrate the fitness-for-purpose of 15 mM IRI in 5 % DMSO as an efficient cryoprotective solution for iPSCs in terms of post-thaw recovery, viability, pluripotency, and transcriptomic changes. This mRNA sequencing dataset has the potential to be used for molecular mechanism analysis relating to cryopreservation. Use of IRIs can reduce DMSO concentrations and its associated toxicities, thereby improving the utility, effectiveness, and efficiency of cryopreservation.

1. Introduction

Induced pluripotent stem cells (iPSCs), reprogrammed from somatic cells can self-renew and differentiate into specialized cell types from all three germ layers (ectoderm, mesoderm and endoderm) (Takahashi et al., 2007). Owing to these unique features, iPSCs, iPSC-derived cells, and organoids are important cellular products that can be used in drug screening, disease modelling, and for cell therapies. Robust, efficient, and reproducible cryopreservation protocols are required to provide reliable master and working cell banks, enabling the requisite quality control checks to be performed, whilst maximising post-thaw cell quality. IPSCs can be cryopreserved as colonies or single cells. For single cell formulations, the use of Rho-associated kinase (ROCK) inhibitor Y-27632 supports the survival of dissociated pluripotent stem cells (Watanabe et al., 2007; Martin-Ibañez et al., 2008; Li et al., 2008). Pluripotent stem cells are highly sensitive to cryopreservation, resulting in reduced viability, low reattachment and altered trilineage differentiation capability (Wagh et al., 2011; Uhrig et al., 2022). Reports on cryopreservation of iPSCs state that 30 % to 80 % of cells survive the cryopreservation process (Hunt, 2011).

Cryopreservation is a complex process where all parameters such as ice nucleation temperature, cooling rate, sample volume, and

* Corresponding author at: Integrated Biobank of Luxembourg (IBBL) - Luxembourg Institute of Health (LIH), 1, rue Louis Rech, L-3555 Dudelange, Luxembourg.
E-mail address: kathleen.mommaerts@ibbl.lu (K. Mommaerts).
[1] University of Pittsburgh School of Medicine, Lothrop St, Pittsburgh, PA 15213, United States.
[2] CRBIP, Institut Pasteur, Université Paris Cité, 75015 Paris, France.

https://doi.org/10.1016/j.scr.2024.103583
Received 13 February 2023; Received in revised form 28 June 2024; Accepted 14 October 2024
Available online 18 October 2024

cryoprotectant parameters (such as dimethyl sulfoxide (DMSO) concentration) must be carefully optimized (Chantelle et al., 2013; Wolkers et al., 2021). Most cryoprotectants exhibit cytotoxicity and hence must be carefully removed post-thaw to reduce cellular damage (Awan et al., 2020). Conventional methods for iPSCs cryopreservation use 10 % DMSO as a cryoprotective agent and a slow cooling rate of 1 °C per minute (Li et al., 2018; Crook et al., 2017). A significant cause of cellular damage during cryopreservation results from ice recrystallization which is defined as the growth of large ice crystals at the expense of small ones. Ice recrystallization inhibitors (IRIs) are small molecules that aid the cryoprotective action by maintaining small ice crystal size within a frozen solution (Chantelle et al., 2013; Poisson et al., 2019). IRIs have shown promising results in mitigating cellular damages in pluripotent stem cells (Alasmar et al., 2023; Briard et al., 2016). They are easily synthesized, tuneable, amenable to industrial production, and have been demonstrated not to be cytotoxic (Briard et al., 2016; Deller et al., 2016).

Recent studies have compared the pre- and post-cryopreserved transcriptomic and proteomic profiles of iPSC-derived cells (Mathews et al., 2023; Neaverson et al., 2022; Chirikian et al., 2022; Ali et al., 2018; Kaindl et al., 2019). Our study investigates transcriptomic changes following cryopreservation of iPSCs by slow freezing with IRIs. In addition to the novelty of the tested cryoprotectants, this study is the first to report, to the best of our knowledge, the analysis of mRNA sequencing data from post-thawed iPSC samples that were cryopreserved using IRIs.

2. Material and methods

2.1. Study design

A toxicity screening study was initially performed to select the optimal specific small-molecule IRI and its concentration. The recovery, viability, and apoptosis of three iPSC lines (iPSC-1 to −3) were assessed following incubation of single-cell suspensions in different IRI-containing solutions for 2 h at room temperature (RT) (Table 1). Then, a cryopreservation study was performed to assess the efficiency of including IRIs in the cryoprotectant solutions for iPSC cryopreservation. Three new iPSC lines (iPSC-4 to −6) were cryopreserved as single-cell suspensions and post-thaw characteristics including pluripotency and differential gene expression were assessed (Table 1). The complete dataset used in this study is available here: https://doi.org/10.17881/fpn5-th91.

2.2. Ethical statement

Subjects provided a written informed consent to participate in the study. Skin samples were provided by two study sources: all skin samples, with the exception of the skin sample used to generate iPSC-6, were provided by the Luxembourg Parkinson's study under approval by the National Ethics Board (Comité National d'Ethique de Recherche (CNER), Ref: 201407/13) and Data Protection Committee (Commission Nationale pour la Protection des Données (CNPD), Ref: 446/2017). The skin sample used to generate iPSC-6 was provided by the CRB-CHU Amiens, Biobanque de Picardie (Biobanking Resources Impact Factor: BB-0033–00017) under approval from the Ministère de la Recherche (N° AC-2013–1827). All research was performed in accordance with relevant guidelines/regulations and in accordance with the Declaration of Helsinki.

Table 1
Subject characteristics.

Study	iPSC lines	Gender	Diagnostic	Age[¥] (years)	Passage
Toxicity study	iPSC-1	Male	Idiopathic Parkinson's Disease	68	P6
	iPSC-2	Male	Healthy control	65	P7
	iPSC-3	Male	Healthy control	62	P7
Cryopreservation study	iPSC-4	Male	Healthy control	65	P7
	iPSC-5	Male	Healthy control	72	P7
	iPSC-6	Female	Healthy Control	23	P15

[¥] Age relates to subject age at skin biopsy collection.

2.3. Induced pluripotent stem cells (iPSCs)

Six different iPSC lines were used for the toxicity screening study (iPSC-1 to −3) and the cryopreservation study (iPSC-4 to −6). For the toxicity screening study, three iPSC lines of similar subject characteristics (gender and age at skin biopsy collection) with different pluripotency status were used. In contrast, for the cryopreservation study, iPSC lines of fully pluripotent status with different characteristics were used (Table 1). The pluripotent status was established by molecular and functional assays. Fibroblast isolation, reprogramming, and iPSCs culture for all cell lines, was performed as previously described (Mommaerts et al., 2022). Briefly, fibroblasts were reprogrammed to iPSCs, using a simplicon™ RNA Reprogramming Kit (Millipore, SCR550) following the manufacturer's instructions. Cultures were maintained on Matrigel (Corning, 354277) coated 6-well plates (Thermo Fisher, 140675) in an incubator at 37 °C with 5 % CO_2 in culture media composed of Essential 8™ Medium (Thermo Fisher, A1517001) supplemented with 1 % penicillin–streptomycin (Gibco, 15070). Absence of mycoplasma contamination was confirmed using MycoAlert™ PLUS mycoplasma detection kit (Lonza, LT07-703). All fibroblast lines, prior to reprogramming, were cryopreserved in a solution containing 10 % DMSO without IRIs. All iPSC lines were cryopreserved in CryoStor® CS10 (CS10, Biolife Solutions, 210102) without IRIs prior to their use in this study.

2.4. Toxicity screening study

Seven solutions were assessed for toxicity: a base buffer solution (i) consisting of CryoStor® CSB buffer (BioLife Solutions, 200102) with no IRI and no DMSO; one IRI compound (IRI-I) at three concentrations (ii; 5 mM, iii; 10 mM and iv; 15 mM); a second IRI compound (IRI-II) at one concentration (v; 15 mM); and two commercial cryopreservation solutions. These commercial cryosolutions were CryoStor® CS10 and CryoStor® CS5 (BioLife Solutions, 205102), which consist of CryoStor® CSB buffer containing 10 % and 5 % DMSO respectively. CryoStor® cryopreservation solutions are animal component-free, defined, and cGMP-manufactured. IRIs were dissolved in CryoStor® CSB buffer. Both IRIs evaluated in this study were *N*-aryl-glyconamides, however the specific composition of the IRI solutions is proprietary (Patent No.: US 9,648,869 B2).

IPSC lines were grown to approximately 80 % confluence by visual assessment, harvested by enzymatic treatment (Accutase™, Stem Cell Technologies, 07920), counted with the CASY-cell counter (OLS, 5651719), and pelleted. The 4 °C pre-cooled cryosolutions were added to each pellet to reach a final concentration of one million viable cells per mL. Each sample was aliquoted in 3 equal volumes of 0.5 mL and incubated for 2 h at room temperature (RT) prior to dropwise addition of culture media to dilute out the cryoprotectant. After centrifugation, cells were suspended in culture media and analysed to assess their recovery, viability, and apoptotic levels.

2.5. Cryopreservation study

Based on the results of the toxicity screening study, the IRI compound (IRI-I) was selected to be evaluated at a concentration of 15 mM,

and three cryopreservation solutions were further evaluated: commercial cryosolution CryoStor® CS10 which contains 10 % DMSO (CS10), 15 mM IRI-I in CryoStor® CS5 which contains 5 % DMSO (IRI-I5) and 15 mM IRI-I in CryoStor® CS10 (IRI-I10).

Cryopreservation. IPSC lines were grown to approximately 80 % confluence by visual assessment, harvested by enzymatic treatment (Accutase™), counted with the CASY-cell counter, and pelleted. The pellets were either lysed for future mRNA sequencing analysis, lysed for future qRT-PCR characterization, seeded for pluripotency assessment, or suspended in their respective 4 °C pre-cooled cryosolutions (CS10, IRI-I5 and IRI-I10) to reach a final concentration of one million cells per mL. Cells suspended in CS10 (1 mL) were immediately aliquoted into 1.8 mL cryovials (FluidX, 65–7501) and transferred to a controlled rate freezer. Cells suspended in IRI-containing cryosolutions (1 mL) were incubated for 15 min at RT prior to aliquoting into cryovials and transferred to a controlled rate freezer. The controlled rate freezers (ICE CUBE 14 M−B and ICE CUBE 14S-B, SY-LAB) cooled the samples from 4 °C to −80 °C at 1 °C per min. Ice nucleation was not induced during the freezing process. The cryopreserved cells were transferred and stored four months in the vapour phase of liquid nitrogen. Four vials were cryopreserved for each cryoprotectant and cell line combination.

Thawing. Cryovials were thawed using a digital warming system (ThawStar CFT2, Biocision) then gently transferred into a tube, diluted by dropwise addition of cell culture media, pelleted by centrifugation and the cryoprotectant solutions removed.

Cell culture for mRNA sequencing. Recovery and viability percentages were assessed ($n = 3$ vials) then the iPSCs were cultured in the previously described media but with the addition of 10 μM ROCK inhibitor Y-27632 (Stem Cell technologies, 72302). After 23 h, a media exchange was performed with culture medium without ROCK inhibitor and a phase-contrast image was taken using phase-contrast microscopy (Leica DMIL LED microscope). One hour later (24 h post-thaw), confluence of iPSCs were assessed with a Cytonote lens-free video microscope (Iprasense) then the cells lysed with QIAzol Lysis Reagent (Qiagen) for mRNA sequencing.

Cell culture for pluripotency assessment. Pluripotency assessment ($n =$ 1 vial) using immunofluorescence and qRT-PCR was performed after 2 passages and 3 to 5 days culture for colony formation. Cell culture media was as above, with ROCK inhibitor present for the first 24 h after initial thawing and each passage.

2.6. Recovery, viability, and apoptosis assessment

Recovery and viability of iPSCs were assessed using a Cellometer Auto 2000 Cell Profiler (Nexcelom Bioscience) and Cellometer AOPI staining solution (Nexcelom Bioscience, CS2-0106). Recovery was calculated using the formula: recovery (%) = (yield of viable cells after thawing/yield of viable cells before cryopreservation)*100. Cell apoptosis was assessed by flow cytometry using the FITC Annexin V Apoptosis Detection Kit 1 (BD Pharmingen, 556547) according to the manufacturer's instructions on a BD FACSVerse. In this kit, single propidium iodide (PI)-stained cells are reported as "necrotic", single Annexin V-stained cells as ''early apoptotic'', double Annexin V/PI-stained cells as "late apoptotic'' cells, and double negative-stained cells as "viable".

2.7. Pluripotency assessment

The self-renewal capability and the trilineage differentiation capability (ability of the iPSC lines to differentiate into ectoderm, mesoderm, and endoderm) were determined. For both capabilities, immunofluorescence (IF) images of 4 % paraformaldehyde-fixed cells were taken using an Axio Observer.Z1 microscope (Zeiss) and qRT-PCR was performed using unfixed cells. Consistency in colony morphology was assessed using phase-contrast microscopy.

Immunofluorescence. For self-renewal capability, the IF primary antibodies targeted SSEA4 (Millipore, MAB4304, 1:25), NANOG (Millipore, AB5731, 1:100), TRA-1–60 (Millipore, MAB4360, 1:25), OCT4 also known as POU5F1 (Abcam, ab19857, 1:600), TRA-1–81 (Millipore, MAB4381, 1:25) and SOX2 (Abcam, ab97959, 1:200). Secondary antibodies included anti-mouse Alexa Fluor 488 and anti-rabbit Alexa Fluor 568 (Invitrogen, A21202 and A10042 respectively, 1:1000). A nuclei counterstain, Hoechst 33,342 (Thermo Fisher, H3570, 1:10 000), was included. To assess trilineage differentiation capability, cells were differentiated as previously described (D'Amour et al., 2005; Sa and McCloskey, 2012; Chambers et al., 2009). Primary IF antibodies targeted β-Tubulin (TUBB3, BD Biosciences, 560338, 1:10) for ectoderm, α-smooth muscle actin antibody (α-SMA, Abcam, ab5694, 1:100) for mesoderm, and SOX17 (R&D Systems, IC19241G, 1:13) for endoderm. The nuclei counterstain was also performed.

Gene expression analysis qRT-PCR. For gene expression analysis, RNA was isolated from QIAzol-lysed cells using the miRNeasy Mini kit (Qiagen, 217004) with on-column DNase treatment. For each sample, one microgram of total RNA (quantified with a Synergy MX (BioTek) spectrophotometer) was reverse-transcribed using the High Capacity Reverse Transcription Kit (Life Technologies, 4374966). qPCR was performed using the microarray TaqMan® hPSC Scorecard Panel kit (Thermo Fisher, A15871), which contains 94 pluripotency and trilineage differentiation genes (Tsankov et al., 2015). The reactions were run on an ABI 7500 Fast Real-Time PCR System and Cqs calculated by 7500 System SDS software *v*2.3 (both Applied Biosystems). Cqs were then uploaded to the hPSC Scorecard™ Analysis Software (Thermo Fisher), which compares the gene expression profile of the sample to that from a reference dataset, defining its pluripotency and trilineage differentiation as positive, borderline or negative.

2.8. mRNA sequencing

RNA was isolated with the Qiagen miRNeasy Mini kit with on-column DNase treatment. RNA concentration were measured with the Quant-IT RiboGreen® RNA Assay Kit (Thermo Fisher, R11490) with a Synergy MX spectrophotometer. RNA quality was assessed using RNA Integrity Numbers (RINs) generated using RNA 6000 Nano Chips running on a 2100 Bioanalyzer (Agilent Technologies). RINs range from 1 (RNA completely degraded) to 10 (RNA completely intact).

RNA sequencing was conducted at CeGaT (Center for Genomics and Transcriptomics, Tübingen, Germany) using a NovaSeq 6000 and 200 ng of RNA. The TruSeq Stranded mRNA kit (Illumina) was used to prepare the library. Two times 100 base pair reads were generated per library. Demultiplexing of the sequencing reads was performed with Illumina bcl2fastq *v*2.20. Adapters were trimmed with Skewer *v*0.2.2. The quality of FASTQ files was analysed with FastQC *v*0.11.5-cegat.

The generated sequencing reads were mapped against the human genome build hg38 using STAR aligner (Dobin et al., 2013) and the read counts for each gene were calculated using featureCounts. Gene expression was normalized by DESeq2 *v*1.22.2 with variance-stabilizing transformation (VST) (Love et al., 2014) and the low expression genes with total counts across all samples less than 10 were excluded. Unsupervised hierarchical clustering of RNA sequencing data with fold change (FC) $\geq$ 1.5 times was conducted using the dist R function. A heatmap was generated using the pheatmap and gplots R packages.

The differential gene expression analysis between 24 h post-thaw cells and their controls (freshly isolated, unfrozen iPSC samples) was performed using DESeq2 with the *p*-value cut-off of 0.01. The dataset was analysed by identifying the common genes that were $>$ 3.0 times deregulated. To do so, any gene that was $>$ 3.0 times deregulated in each cryosolution was included. This was performed for each of the cell lines separately. Then, for each cryosolution, deregulated genes common to all three cell lines were identified. Our logic was that the identified genes are susceptible to deregulation in the specified cryosolution as a consequence of the cryopreservation process itself, independent of the cell line's identity.

Pathway identification was performed with Gene Set Enrichment Analysis (GSEA) using the knowledge based Molecular Signatures Database (mSigDB) (Subramanian et al., 2005). Fisher's exact test was performed to identify the statistical enrichment of the categories in mSigDB using the differentially up- or down-regulated genes as the test set. All detected genes were taken as the background set. Categories with an adjusted *p*-value (*p* adj) < 0.01 and containing at least five differentially expressed genes (DEGs) were considered significantly enriched.

Pathways relating to pluripotency, apoptosis induction, hypoxia, stress-induced, and membrane transport were selected for further analysis. The keywords to select the pathways of interest for pluripotency were ESC, PLURI, EMBRYONIC; for apoptosis: APOP, TNF, FAS, CASP; for hypoxia: HYPOX, OSMO; for any stress: STRESS, and for membrane transport: …MEMBRANE…TRANSPORT. Venn diagrams were generated using https://bioinformatics.psb.ugent.be/webtools/Venn/.

2.9. Statistical analysis

For the toxicity screening and cryopreservation study, a two-way ANOVA was used for data analysis. When treatments were significantly different ($p < 0.05$), a Holm-Sidak test for pairwise comparisons was performed. All analysis were performed using SigmaPlot *v*12.5 (Systat). Normality was tested using the Shapiro–Wilk test. All graphs were done in Excel version 2003.

3. Results

3.1. Toxicity screening study

Initially, a toxicity screening study was performed to determine which of the IRI compounds to use in the cryopreservation study.

Pluripotency Assessment. Based on the immunofluorescence (Fig. 1A) and molecular assay results (Fig. 1B and 1C), we concluded that the pluripotency status of iPSC-1 was "not pluripotent", iPSC-2 was "pluripotent", and iPSC-3 was "borderline". At the morphological level,

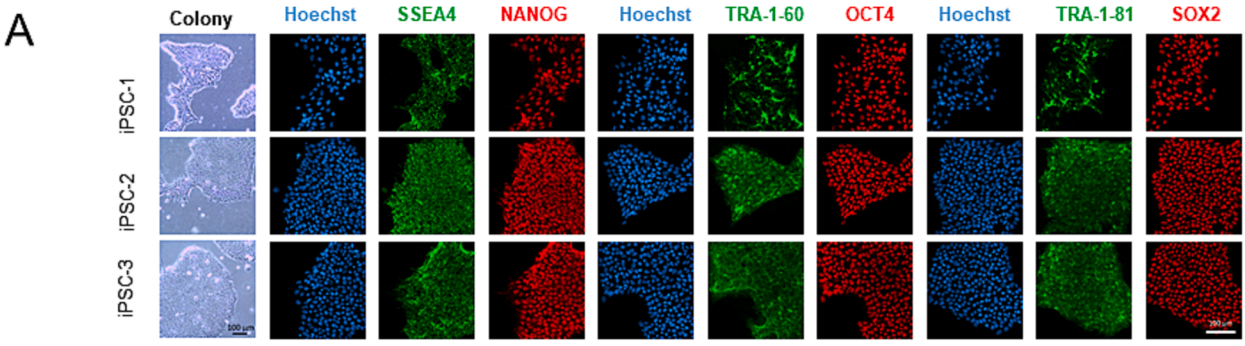

B

	Undifferentiated cells			
	Self-renew	Ecto	Meso	Endo
iPSC-1	-	-	-	-
iPSC-2	+	-	-	-
iPSC-3	B	-	-	-

C

	Differentiated cells			
	Self-renew	Ecto	Meso	Endo
iPSC-1	-	B	+	-
iPSC-2	-	+	+	-
iPSC-3	-	+	+	-

D

Analysis	Results measured as	iPSC line	Solutions i Base buffer CSB	ii IRI-I 5mM	iii IRI-I 10mM	iv IRI-I 15mM	v IRI-II 15mM	CS5 CS5	CS10 CS10	Cell line comparison Mean
Recovery (%)	AOPI staining intensity	iPSC-1	62.0 ± 12.1	83.9 ± 3.6	69.0 ± 12.0	76.7 ± 12.0	81.6 ± 14.4	72.3 ± 5.6	62.3 ± 5.9	72.6 ± 8.7*** iPSC-2/-3
		iPSC-2	48.2 ± 3.6	45.5 ± 16.6	60.0 ± 9.6	41.5 ± 3.2	37.9 ± 4.0	49.7 ± 8.6	52.2 ± 13.6	47.9 ± 7.2*** iPSC-1
		iPSC-3	43.7 ± 23.5	60.2 ± 2.3	47.3 ± 12.4	48.8 ± 15.5	56.2 ± 5.0	55.9 ± 8.6	48.7 ± 13.6	51.5 ± 5.9*** iPSC-1
		Mean	51.3 ± 9.6 #	63.2 ± 19.4#	58.8 ± 10.9#	55.7 ± 18.6#	58.6 ± 22.0#	59.3 ± 11.7#	54.4 ± 7.1 #	
Viability (%)	AOPI staining intensity	iPSC-1	70.6 ± 2.6	73.4 ± 8.5	73.3 ± 5.8	80.6 ± 2.0	80.4 ± 6.5	77.6 ± 4,2	73.6 ± 9.3	75.6 ± 3.9*** iPSC-3
		iPSC-2	70.5 ± 6.6	78.1 ± 9.9	85.0 ± 1.9	79.0 ± 4.3	77.1 ± 2.5	78.0 ± 3.2	76.5 ± 4.1	77.7 ± 4.2*** iPSC-3
		iPSC-3	80.6 ± 5.0	89.0 ± 2.1	83.1 ± 6.9	88.0 ± 0.3	84.8 ± 0.8	85.8 ± 3.2	84.1 ± 6.4	85.1 ± 2.9*** iPSC-1/-2
		Mean	73.9 ± 5.8 *iv	80.2 ± 8.0 #	80.5 ± 6.3 #	82.5 ± 4.8 *i	80.8 ± 3.9 #	80.5 ± 4.6 #	78.1 ± 5.5 #	
Viability (%)	Flow cytometry of Annexin V and PI stained cells	iPSC-1	78.6 ± 4.7	77.2 ± 1.9	76.2 ± 2.3	74.8 ± 1.0	75.2 ± 1.5	71.9 ± 1.9	73.2 ± 1.2	75.3 ± 2.3*** iPSC-2
		iPSC-2	66.5 ± 1.6	73.0 ± 3.9	72.2 ± 1.9	72.5 ± 2.5	72.5 ± 1.2	68.6 ± 6.5	64.8 ± 6.8	70.0 ± 3.4*** iPSC-1/-3
		iPSC-3	67.8 ± 4.3	75.0 ± 1.4	73.7 ± 3.3	74.0 ± 1.5	77.3 ± 2.9	73.3 ± 4.5	73.4 ± 2.6	73.5 ± 2.9*** iPSC-2
		Mean	71.0 ± 6.7 #	75.1 ± 2.1 #	74.0 ± 2.1 #	73.8 ± 1.2 #	75.0 ± 2.4 #	71.2 ± 2.4 #	70.5 ± 4.9 #	

Fig. 1. Pluripotency assessment (A-C) of the three iPSC lines (iPSC-1, −2, and −3) and toxicity screening study results (D) following room temperature incubation of single-cell suspension in 7 solutions: a base buffer solution (i; with no IRI and no DMSO), two IRIs compounds at three concentrations (ii; 5 mM, iii; 10 mM and iv,v; 15 mM) and two commercial cryopreservation solutions (CryoStor® CS10, and CryoStor® CS5). (A) Phase-contrast photograph of colonies, along with immunostainings for pluripotency markers (SSEA4, NANOG, TRA-1–60, OCT4, TRA-1–81 and SOX2). All cultures were stained simultaneously and all photographs were taken using the same microscope settings. Scale bar is shown at the bottom right and depicts 100 μm. (B, C) Microarray TaqMan® hPSC Scorecard results for self-renewal and trilineage differentiation genes of undifferentiated cells (B) and differentiated (C) cells, respectively. Scorecard result icons "+" (positive), "B" (borderline), or "–" (negative) are displayed and color coded green (self-renewal), blue (ectoderm), orange (mesoderm), and purple (endoderm). (D) Performance results (mean ± 1 standard deviation) for recovery and viability of the three technical replicates. # denotes no statistically significant difference between any group, *$p < 0.05$ and **$p < 0.001$. (For interpretation of the references to color in this figure legend, the reader is referred to the web version of this article.)

cell lines iPSC-2 and iPSC-3 grew in typical rounded colonies with defined borders, whilst iPSC-1 had typical morphology at the centre of the colonies but abnormal star-shaped cells on the border (Fig. 1A, Colony). Concerning the pluripotency immunostaining for SSEA4, NANOG, TRA-1–60, OCT4, TRA-1–81 and SOX2, iPSC-2 and iPSC-3, but not iPSC-1, stained positively for SSEA4, TRA-1–60 and TRA-1–81 (Fig. 1A). For the gene expression profile of undifferentiated cells using the TaqMan® hPSC Scorecard Panel kit (94 genes), iPSC-2 was classified as "pluripotent", iPSC-3 as "borderline" and iPSC-1 as "not pluripotent" (Fig. 1B). In the gene expression profiling using differentiated cells, all three cell lines expressed the genes associated with the mesoderm germ layer and none expressed genes associated with the endoderm germ layer; for the genes typically associated with the ectoderm germ layer, iPSC-1 had borderline expression whilst iPSC-2 and iPSC-3 had positive expression (Fig. 1C).

Recovery. There were no statistically significant differences in recovery, measured via AOPI staining intensity, between any of the cryosolutions (i to v, CS5 and CS10), with mean recovery across the three iPSC lines ranging between 51.3 % (i) and 63.2 % (ii) (Fig. 1D). Mean recovery was higher in iPSC-1 (72.6 %) than iPSC-2 (47.9 %) and iPSC-3 (51.5 %) ($p < 0.001$) but the difference between iPSC-2 and iPSC-3 was not statistically significant ($p = 0.294$).

Viability. No statistically significant differences in viability, measured via AOPI staining intensity, were found between any of the cryosolutions, aside from IRI solution iv, which showed a higher viability than the buffer control i (mean 82.5 % and 73.9 % respectively, $p = 0.032$) (Fig. 1D). Mean viability was higher in iPSC-3 (85.1 %) than iPSC-1 (75.6 %) and iPSC-2 (77.7 %) ($p < 0.001$). There was no statistically significant difference in viability and early apoptosis, measured via flow cytometry of Annexin V and PI stained cells, between any of the cryosolutions, with mean viability across the three iPSC lines ranging between 70.5 % (CS10) and 75.1 % (ii) (Fig. 1D and Fig. S1). Mean viability was lower in iPSC-2 (70.0 %) than iPSC-1 (75.3 %) and iPSC-3 (73.5 %) ($p < 0.001$). The cryosolutions showed an enrichment in respect of late apoptosis and necrosis for each specific cell line with the highest percentages in the cell line iPSC-2 assessed as "pluripotent" (mean 9.3 % and 0.4 % respectively) (Fig. S1).

Taking all of the above into account, we selected cryosolution iv (15 mM IRI-I in Cryostor® CSB) for our cryopreservation study because it had the highest mean viability (by AOPI staining intensity) for all the cell lines and comparable recovery (by AOPI staining intensity) and viability (by flow cytometry of Annexin V and PI stained cells) to the other IRI-containing cryosolutions.

3.2. Cryopreservation study

Results of the cryopreservation study are presented as follows: assessment of pluripotency status prior to cryopreservation, post-thaw characteristics and differential gene expression. New cell lines (iPSC-4 to −6), different from those used in the toxicity screening study (iPSC-1 to −3), were used.

3.2.1. Pluripotency assessment prior to cryopreservation

Based on the immunofluorescence and molecular assay results, all iPSC lines (iPSC-4 to −6) were considered pluripotent (Table 2). The results for each pluripotency characterization assay in each cell line are shown in Fig. S2. At the morphological level, all iPSC lines grew in typical rounded colonies with defined borders (Table 2 and Fig. S2A, Colony). All cell lines showed positive pluripotency immunostaining for SSEA4, NANOG, TRA-1–60, OCT4, TRA-1–81 and SOX2 (Table 2 and Fig. S2A). All lines expressed genes typically associated with pluripotency, with no signal associated with differentiation in the three germ layers (Table 2 and Fig. S2B). Once differentiated, all three cell lines expressed genes typically associated with the germ layers ectoderm and mesoderm (Fig. S2C). All lines were capable of differentiation into the endoderm germ layer as shown by positive immunostaining for SOX17 (Fig. S2D).

3.2.2. Post-thaw characteristics

Recovery. The mean cell recovery, measured via AOPI staining intensity, in cryosolution IRI-I5 (64.1 %) was higher than in IRI-I10 (49.2 %, $p = 0.021$) and in CS10 (51.2 %, $p = 0.035$)(Fig. 2A). The difference between IRI-I10 and CS10 was not statistically significant. Mean recovery was higher in iPSC-4 (63.0 %) than iPSC-6 (46.8 %, $p = 0.012$).

Viability. The viability, measured via AOPI staining intensity, prior to cryopreservation was 89.7 ± 0.8 % for all cell lines. The mean post-thaw viability of cells in cryosolution IRI-I5 (85.3 %) was higher than IRI-I10 (80.7 %, $p = 0.037$)(Fig. 2A). Mean viability was higher in iPSC-5 (86.1 %) than iPSC-6 (81.4 %, $p = 0.03$).

Confluence. The confluence, 24 h post seeding, measured with a Cytonote, was already radically different between the cell lines and cryosolutions, ranging from 8 % (iPSC-5, IRI-I10) to 74 % (iPSC-4, CS10)

Table 2
Pluripotency assessment (self-renewal and trilineage differentiation capability) by immunofluorescence (IF) and qRT-PCR of three iPSC lines (iPSC-4, −5 and −6) used in the cryopreservation study (prior to cryopreservation and post expansion). "+" denotes a positive expression, "-" denotes a negative expression, "B" stands for borderline expression and "NA" denotes not tested.

			Prior Cryopreservation			Post expansion					
			iPSC-4	iPSC-5	iPSC-6	iPSC-4			iPSC-6		
						CS10	IRI-I5	IRI-I10	CS10	IRI-I5	IRI-I10
Pluripotency	**Colony**		+	+	+	+	+	+	+	+	+
	IF	**SSEA4**	+	+	+	+	+	+	+	+	+
		Nanog	+	+	+	+	+	+	+	+	+
		TRA-1–60	+	+	+	+	+	+	+	+	+
		Oct4	+	+	+	+	+	+	+	+	+
		TRA-1–81	+	+	+	+	+	+	+	+	+
		SOX2	+	+	+	+	+	+	+	+	+
	qRT-PCR	**Self-renew**	+	+	+	+	+	+	+	+	+
		Ecto	−	−	−	−	−	−	−	−	−
		Meso	−	−	−	−	−	−	−	−	−
		Endo	−	−	−	−	−	−	−	−	−
Trilineage differentiation	**qRT-PCR**	**Self-renew**	−	−	−	NA	NA	NA	NA	NA	NA
		Ecto	+	B	+	NA	NA	NA	NA	NA	NA
		Meso	+	+	+	NA	NA	NA	NA	NA	NA
		Endo	−	−	−	NA	NA	NA	NA	NA	NA
	IF	**Ecto**	NA	NA	NA	+	−	−	+	+	+
		Meso	NA	NA	NA	+	+	+	+	+	−
		Endo	+	+	+	+	+	+	+	+	+

A

Analysis	iPSC line	Cryosolutions: CS10		IRI-I5 (15 mM IRI-I in CS5)		IRI-I10 (15 mM IRI-I in CS10)		Cell line comparison: Mean	
Recovery (%)	iPSC-4	60.9 ± 6.0		76.7 ± 11.5		51.5 ± 10.3		63.0 ± 12.7	*iPSC-6
	iPSC-5	51.3 ± 3.3		54.0 ± 7.6		58.7 ± 16.8		54.7 ± 3.7	#
	iPSC-6	41.6 ± 10.1		61.5 ± 8.1		37.3 ± 13.7		46.8 ± 12.9	*iPSC-4
	Mean	51.2 ± 9.7	*IRI-I5	64.1 ± 11.6	*CS10, IRI-I10	49.2 ± 10.9	* IRI-I5		
Viability (%)	iPSC-4	82.9 ± 2.7		86.3 ± 1.5		79.3 ± 4.9		82.9 ± 3.5	#
	iPSC-5	87.4 ± 4.6		84.6 ± 1.3		86.3 ± 3.8		86.1 ± 1.4	*iPSC-6
	iPSC-6	82.7 ± 5.0		84.9 ± 2.9		76.5 ± 2.2		81.4 ± 4.3	*iPSC-5
	Mean	84.3 ± 2.6	#	85.3 ± 0.9	*IRI-I10	80.7 ± 5.0	*IRI-I5		

B

	Confluence (%)		
	CS10	IRI-I5	IRI-I10
iPSC-4	74	61	24
iPSC-5	25	21	8
iPSC-6	50	53	36

C

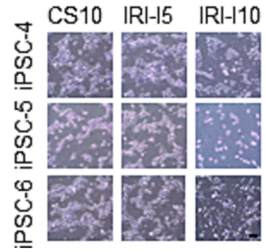

Fig. 2. Post-thaw assessment in the cryopreservation study where the cryoprotective efficiency of two IRI-containing cryosolutions (IRI-I5: 15 mM IRI-I in 5 % DMSO-containing solution and IRI-I10: 15 mM IRI-I in 10 % DMSO-containing solution) were compared with CryoStor® CS10 (CS10) using three iPSC lines (iPSC-4, −5 and −6). (A) Performance results (mean ± 1 standard deviation) for post-thaw recovery and viability of the three technical replicates. # denotes no statistically significant difference between any group, *$p < 0.05$.(B) Confluence measurement 24 h post-thaw after expansion of the iPSC lines. (C) Phase-contrast images after media exchange 23 h post-thaw. Scale bar is shown at bottom right and depicts 100 μm.

(Fig. 2B). At 24 h post seeding, visual observations of iPSC-5 showed a lower confluence than iPSC-4 and iPSC-6 (Fig. 2C). It was also observed, in the iPSC-5 and IRI-I10 combination, there were fewer adherent cells. This low density is not a seeding error as the number of cells floating in solution was higher.

RNA yield and quality. RNA yield per well correlated with the visual confluence of cells, ranging from 0.7 μg (iPSC-5, IRI-I10) to 13.0 μg (iPSC-6, CS10). RNA integrity, determined using a Bioanalyzer, was very high in all samples, with RIN values of 9.5 (iPSC-5, IRI-I10), 9.7 (iPSC-6, IRI-I5) and 10.0 (all remaining samples) denoting undegraded RNA.

Pluripotency assessment. The pluripotency assessment was performed for the surviving cells after 2 passages. IPSC-5 cells cryopreserved with IRI-I10 did not survive the thawing process, whilst those cryopreserved in CS10 and IRI-I5 did not survive the first passage. After 2 passages, based on the immunofluorescence and molecular assay results, iPSC-4 and iPSC-6 cryopreserved with CS10, as well as iPSC-6 cryopreserved with IRI-I5, were pluripotent (Table 2). IPSC-4 cryopreserved with IRI-I5 and IRI-I10 as well as iPSC-6 with IRI-I10 were determined as borderline. The results for each pluripotency characterization assay in each cell line are also shown in Fig. S3. At the morphological level, both surviving iPSC lines (iPSC-4 and iPSC-6) grew in typical rounded colonies with defined borders (Fig. S3A, Colony). All showed positive pluripotency immunostaining for SSEA4, NANOG, TRA-1–60, OCT4, TRA-1–81 and SOX2 (Fig. S3A). Both lines expressed genes typically associated with pluripotency, with no signal typically associated with differentiation in the three germ layers (Fig. S3B). For iPSC-4, negative expression of the ectoderm target TUBB3 was obtained with IRI-I5 and IRI-I10 (Fig. S3C). For iPSC-6, negative expression of the mesoderm target α-SMA was obtained with IRI-I10. The remaining samples were capable of differentiating into each of the three germ layers as shown by positive immunostaining for ectoderm (TUBB3), mesoderm (α-SMA), or endoderm (SOX17).

3.2.3. Differential gene expression

Heatmap analysis. Heatmap of the deregulated genes (p adj ≤ 0.05 and fold change (FC) ≥ 1.5) showed that the iPSC lines post cryopreservation clustered together, with different gene expression patterns than their counterparts prior to cryopreservation (Fig. 3A). Each genotype exhibited strong similarities regardless of the cryosolution used but there was less differential clustering between the pre- and post-cryopreserved condition than between genotypes, suggesting that cryopreservation has a stronger effect than the genotype effect.

Gene analysis. A Q30 value of 91.8 % was obtained. Significant differences between pre- and post-thaw cell lines were seen for 492 genes (p adj ≤ 0.05 and FC > 3.0) (Fig. 3B and Fig. 3C). The highest number of DEGs was observed for IRI-I10 and the lowest for CS10. Of the 10 most prominently up-regulated genes in each cryosolution, the following seven were common to all three cryosolutions: *MT2A*, *SERPINE1*, *NQO1*, *HMOX1*, *VGF*, *RTL5* and *TIMP4* (Fig. S4A). All these genes, with the exception of the unannotated gene *RTL5*, are protein coding with GO annotations including drug and protease binding, oxidoreductase and growth factor activity. The equivalent down-regulated genes were *H1-0*, *NPTX1*, *KLF15*, *AL591742.2*, *SYT7* and *C3* (Fig. S4B). All these genes, with the exception of AL591742.2 (a long non-coding RNA) are protein coding, of which *H1-0* and *NPTX1* are unannotated and the others have GO annotations including DNA-, calcium ion- and signalling receptor-binding.

To confirm that the cryopreserved and thawed iPSC lines remained pluripotent, the expression of the stemness gene markers *KLF4*, *HESX1*, *REST*, *NANOG*, *POU5F1*, *SOX2*, *ZIC3*, *SALL4*, *CXCL5*, *DNMT3B*, *IDO1*, *LCK*, and *TRIM22* were analysed. No differences in expression were found using the common dataset with FC > 3.0. However, when the entire dataset with FC ≥ 1.5 was analyzed, *HESX1* and *DNMT3B* were up-regulated in all three cryosolutions, *ZIC3* and *IDO1* were down-regulated in all three cryosolutions and *NANOG* was up-regulated only for CS10 and IRI-I5. The $\log_2$ (FC) in CS10, IRI-I5 and IRI-I10 was 0.91, 0.94 and 1.06 respectively for *HESX1*, 0.66, 0.65 and 0.59 for *DNMT3B*, −0.66, −0.68 and −0.66 for ZIC3, −1.09, −1.09 and −1.07 for *IDO1*. The $\log_2$ (FC) in CS10 and IRI-I5 was 0.72 and 0.66 for *NANOG*.

Pathway analysis. The lowest number of selected deregulated pathways was obtained for CS10 and the highest for IRI-I10 (Fig. 3D). There were no statistically significant up-regulated pathways for IRI-I5. There was one up-regulated pathway for CS10 (Hallmark_hypoxia), which was common to IRI-I10 (Fig. 3E). The other pathways up-regulated in IRI-I10

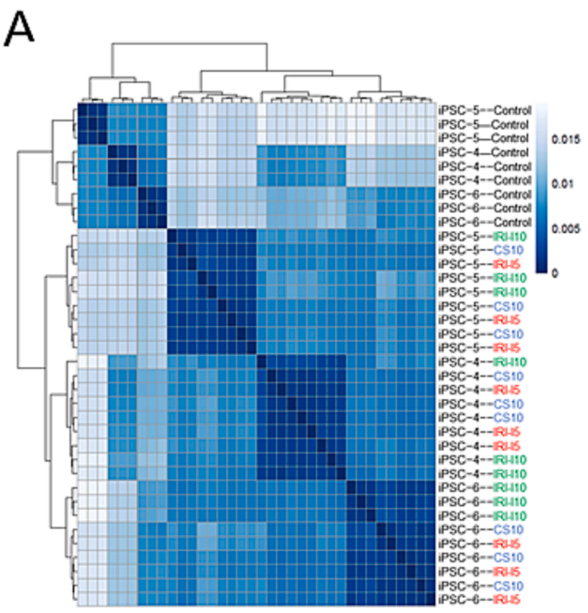

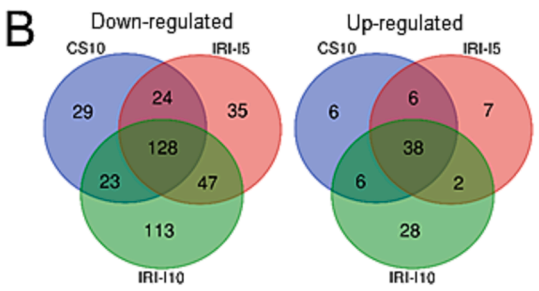

C

Number of DEGs	CS10	IRI-I5	IRI-I10
Down-regulated	204	234	311
Up-regulated	56	53	74
De-regulated	260	287	385

D

Number of selected pathways	CS10	IRI-I5	IRI-I10
Down-regulated	13	18	28
Up-regulated	1	0	9
De-regulated	14	18	37

E

Pathways deregulation	Cryoprotectants	Pathway name
	Common CS10 and IRI-I10	HALLMARK_HYPOXIA
Up-regulated	IRI-I10	CONCANNON_APOPTOSIS_BY_EPOXOMICIN_UP
		HALLMARK_HYPOXIA
		GO_RESPONSE_TO_OXIDATIVE_STRESS
		WINTER_HYPOXIA_METAGENE
		GO_CELLULAR_RESPONSE_TO_STRESS
		GO_EMBRYONIC_MORPHOGENESIS
		GO_REGULATION_OF_RESPONSE_TO_STRESS
		GO_REGULATION_OF_CELLULAR_RESPONSE_TO_STRESS
		BUYTAERT_PHOTODYNAMIC_THERAPY_STRESS_UP
Down-regulated	Common all cryoprotectants	GO_PASSIVE_TRANSMEMBRANE_TRANSPORTER_ACTIVITY
		GO_INORGANIC_ION_TRANSMEMBRANE_TRANSPORT
		GO_ION_TRANSMEMBRANE_TRANSPORT
		GO_METAL_ION_TRANSMEMBRANE_TRANSPORTER_ACTIVITY
		GO_INORGANIC_CATION_TRANSMEMBRANE_TRANSPORTER_ACTIVITY
		GO_REGULATION_OF_TRANSMEMBRANE_TRANSPORT
		GO_TRANSMEMBRANE_TRANSPORT
		GO_CATION_TRANSMEMBRANE_TRANSPORTER_ACTIVITY
		GO_TRANSMEMBRANE_TRANSPORTER_ACTIVITY
		GO_MONOVALENT_INORGANIC_CATION_TRANSMEMBRANE_TRANSPORTER_ACTIVITY

Fig. 3. mRNA sequencing results for deregulated genes and pathways in the cryopreservation study. (a) heatmap of the differentially expressed genes (degs). controls are the ipsc lines prior to cryopreservation. (b) venn diagram of the down-regulated and up-regulated degs. (c) number of degs deregulated. (d) number of deregulated pathways selected for pluripotency, apoptosis induction, hypoxia, stress-induced, and membrane transport. (e) ten most up- and down-regulated selected pathways. the degs are calculated as transcript levels of the ipsc lines (ipsc-4,−5 and −6) following cryopreservation and thawing with different cryosolutions (CS10, IRI-I5 and IRI-I10) as compared to freshly isolated iPSC lines (n = 3). Heatmap analysis was performed using the entire dataset (p adj ≤ 0.05 and fold change (FC) ≥ 1.5) while gene and pathway analysis was performed using the genes deregulated common for each cryosolutions for each cell line assessed separately (p adj ≤ 0.05 and FC > 3.0).

were related to apoptosis, hypoxia, stress, and pluripotency. For the 10 most down-regulated pathways, all pathways were common to all three cryosolutions and were membrane transport-related.

3.3. Summary

In summary, the cryosolution IRI-I5 exhibited the highest post-thaw recovery and viability but the cryosolution CS10 had the lowest number of DEGs and deregulated pathways. However, the differences between these two cryosolutions were generally small in magnitude. IRI-I10 performed significantly poorer than the other cryosolutions, with lower post-thaw recovery and viability rates, and higher numbers of DEGs and deregulated pathways.

4. Discussion

We compared IRI-containing cryosolutions with the commercially available CryoStor® CS10 for cryopreservation of iPSCs. First, a toxicity screening study was performed which identified the optimal small-molecule IRI solution iv (15 mM IRI-I in CryoStor® CSB). Then, a

cryopreservation study compared the cryoprotective efficiency of CryoStor® CS10 (which contains 10 % DMSO) with 15 mM IRI-I in CryoStor® CSB solution either containing 5 % or 10 % DMSO.

The initial toxicity screening study demonstrated that the IRI-containing solutions were no more membrane-disrupting or apoptosis-inducing than the DMSO-based solutions after 2 h exposure at RT; there were no differences in recovery and viability between the IRI containing solutions to the base buffer CryoStor® CSB, or to the CryoStor® CS10 and CS5 controls. There was only one exception, where the base buffer demonstrated lower viability results compared to the IRI-containing solution iv (15 mM IRI-I in CryoStor® CSB). Post-incubation, iPSC-2 showed lower recovery and viability compared to iPSC-1 and iPSC-3. Given that the iPSC lines were of similar subject characteristics, we assign the higher sensitivity of iPSC-2 to its fully pluripotent status.

In the cryopreservation study, the cryosolutions IRI-I5 and CS10 outperformed IRI-I10 and had very similar numbers of DEGs (a difference of 1.9 % in the entire dataset with FC $\geq$ 1.5). The difference between the two IRI-containing cryosolutions is the DMSO content, with 10 % and 5 % in IRI-I10 and IRI-I5 respectively. We assign the reduced cryoprotective efficiency of IRI-I10 to a negative interaction between the IRI compounds and the higher DMSO content. This is consistent with published data where DMSO has been shown to modulate intracellular IRI activity (William and Acker, 2020).

Post-thaw, iPSC-5 showed an intermediate recovery and the highest viability which contradicts the visual appreciation and expansion failure at 24 h. This anomaly is supported by published data, where post-thaw assessments of cryopreservation outcome performed within 1 h of thawing yielded overestimates in survival, due to both apoptotic and necrotic processes that lead to cell death following cryopreservation (Baust et al., 2000; Baust et al., 2001). In embryonic stem cells (ESCs), previous studies showed a high viability post-thaw, then a rapid decline to 30 % viability within 90 min, due to apoptosis (Wagh et al., 2011; Heng et al., 2006). The iPSC-5 cell line showed higher sensitivity to cryopreservation and post-cryopreservation passage than iPSC-4 and iPSC-6. The pluripotency status of iPSC-5 was equivalent to iPSC-4 and iPSC-6, and its cell line characteristics similar to iPSC-4, hence the higher sensitivity is due to currently unknown individual cell line specificities.

Our transcriptomic analysis compared 24 h post-thaw iPSCs and their freshly isolated (unfrozen) iPSC sister samples. In agreement with our study, a previous transcriptomic analysis performed with human ESCs cryopreserved using a 10 % DMSO cryosolution found a higher number of down-regulated than up-regulated DEGs (Wagh et al., 2011). The authors demonstrated that these DEGs are controlled in a time-dependent manner with the number of the frozen-thawed specific genes upregulated reaching a maximal plateau within 24 h and dropping down at 48 h.

Multiple pathways of apoptosis initiation are involved in cryopreservation failure (Baust et al., 2001; Baust et al., 2002). In our study, two factors had an apoptosis-inhibitory effect. Firstly, ROCK inhibitor was present in the culture medium for 23 h following seeding of the iPSCs (Narumiya et al., 2000). A previous study demonstrated that ROCK inhibition following cryopreservation inhibits caspase-8 activity (Xu et al., 2010). Secondly, CryoStor® CS5 and CS10 contain a caspase-1 inhibitor in addition to DMSO, which is also an apoptosis inhibitor (Baust et al., 2000). In our study, no caspase DEGs were identified using the common dataset with FC > 3.0. However, when using the entire dataset with FC $\geq$ 1.5, the different cryosolutions showed similar low levels of *CASP3* and *CASP8* up-regulation and *CASP10* down-regulation. Given that the expression levels of these caspases were similar in all three cryosolutions, this suggests that none of them had a particularly unique effect on those genes.

A primary goal in iPSC cryopreservation is minimizing pluripotency alterations resulting from the cryopreservation protocols and reagents. For example, cryopreservation of human ESCs with 10 % DMSO had resulted in a reduced OCT4 marker expression (Katkov et al., 2006). In our study, the expression levels of the stemness genes were similar in all three cryopreservation solutions, which suggests that none of the cryosolutions had a particularly unique effect on those genes. This is further supported by the low coefficient of variation ($\leq$ 3 %) obtained between the cryosolutions for the self-renewal genes included in the TaqMan® hPSC Scorecard microarray (*CXCL5*, *DNMT3B*, *HESX1*, *IDO1*, *LCK*, *NANOG*, *POU5F1*, *SOX2*, and *TRIM22*). This is not consistent with a study where down-regulation of DEGS of stemness genes (*KLF4*, *HESX1*, *REST*, *NANOG*, *POU5F1*, *SOX2*, *ZIC3*, *SALL4*) was demonstrated at 24 h post-thaw for human ESCs cryopreserved using a different 10 % DMSO cryosolution (Wagh et al., 2011).

A previous study has investigated the effect of cryopreservation of iPSCs (using both conventional slow-freezing and adherent vitrification) on gene expression (Kaindl et al., 2019). Similarly to our study, RNA sequencing was performed on cells immediately prior to and one-day post thawing, and these authors additionally analysed cells 4 days post thaw. Their results differ from ours in that they found neither cryopreservation process to have a discernible effect on DEG. This difference may be due to the use of different thresholds to report DEGs, in terms of numbers of reads.

In our transcriptome analysis, many pathways, potentially linked to the cryopreservation process, were found deregulated. It is unclear which changes in gene expression are protective or detrimental to the cells. In order to decipher the impact of these changes, we investigated the specific pathways that were deregulated only in IRI-I10 (the cryopreservation solution that caused the most deregulation). In these pathways, 19 DEGS that were deregulated in the common dataset with FC > 3.0 were identified.

From this list, the 10 genes *HSPA6*, *FLNC*, *MAP1A*, *SLC1A4*, *SLC22A3*, *DHRS2*, *TLR4*, *SERPINB3*, *SPP1* and *EDN1* were up-regulated only in IRI-I10. The function of these genes fell into different functional categories that are important for cell survival. The up-regulation of the heat shock protein *HSPA6* has been associated with protection from apoptosis (Beere et al., 2000). *FLNC* codes for filamin C, an actin binding protein, while *MAP1A* codes for microtubule-associated protein 1A (Stossel et al., 2001; Hirokawa, 1994). Both proteins are closely associated with the stabilization of the cytoskeleton. *SLC1A4* and *SLC22A3* code for the solute carrier family 1 member 4 and solute carrier family 22 member 3 respectively, and are part of the solute carrier (SLC) superfamily, which are membrane transport proteins (Arriza et al., 1993). Up-regulation of *DHRS2*, that code for the enzyme dehydrogenase/reductase SDR family member 2, has been shown to protect against apoptosis induced by oxidative stress-mediated cellular injury (Monge et al., 2009). *TLR4* codes for the Toll-like receptor 4, which is a key receptor for activating the innate immune system. In platelets, cryopreservation did not change the surface abundance of TLR4 (Wood et al., 2021). Up-regulation of *SERPINB3*, which codes for serpin family B member 3, significantly attenuates apoptosis (Vidalino et al., 2009). The roles of the genes *SPP1* that codes for Secreted Phosphoprotein 1 and *EDN1* that codes for Endothelin 1 remain unknown. We found that the up-regulated genes present only in IRI-I10-cryopreserved cells are mainly associated with the stem cell membrane and apoptosis.

The 8 genes *NQO1*, *HMOX1*, *SERPINE1*, *ANXA1*, *MT1E*, *MT2A*, *CALCA* and *FOXA2* were up-regulated in all the cryosolutions. *NQO1* codes for a NAD(P)H quinone oxidoreductase, which protects against oxidative stress (Dinkova-Kostova and Talalay, 2010). The up-regulation of *HMOX1*, which works mainly as an antioxidant protein, is a major defense mechanism against oxidative stress and tissue injury (Yoshida et al., 2001). *SERPINE1* codes for plasminogen activator inhibitor 1 (PAI-1). The gene was found up-regulated in neural stem cells in the hypoxic group compared with the control group (Shi et al., 2018). The *ANXA1* gene, which codes for Annexin A1, has anti-inflammatory activity (Sugimoto et al., 2016). *MT1E* and *MT2A* are both metallothioneins (MTs) which have potential protective effects against oxidative stress (Babula et al., 2012). *CALCA*, which codes for

calcitonin-related polypeptide alpha, has been associated with various roles including calcium homeostasis, regulation of the immune response and cell proliferation as well as apoptosis after tissue injury (Russell et al., 2014). Recently, *CALCA* has also been identified as a regulator of stem cell self-renewal and differentiation (Lv et al., 2022). The role of the gene *FOXA2* (which codes for forkhead box A2) with regards to cryopreservation is unclear. As these 8 DEGs identified in all three cryosolutions are associated with protective action, we can conclude that the up-regulation is linked with the cryopreservation process, regardless of the cryosolution.

It is noteworthy that in our transcriptome analysis a pathway related to hypoxia was associated with CS10 and IRI-I10, but not IRI-I5. This difference only concerned the gene *CAV1*, as the other genes (*SERPINE1*, *HMOX1*, *MT1E* and *MT2A*) were up-regulated for all three cryosolutions. *CAV1* codes for caveolin-1, which is a cholesterol-binding protein that can potentially regulate a variety of cellular processes including apoptosis (Xu et al., 2016). Caveolae are mechanosensitive and *CAV1* expression has been closely linked with stem cell fate and differentiation (De Belly et al., 2022). The similar levels of caveolin up-regulation in our cryosolutions suggests a protective action linked with the cryopreservation process, regardless of the cryosolution.

A limitation of this study is that we are unable to say whether the higher post-thaw recovery and viability is due to the addition of IRI or to the reduction in DMSO concentration from 10 % to 5 % as no CryoStor® CS5 was included in the study. It has been found that in iPSCs, a 15 % to 50 % increase in recovery and viability occurred when DMSO concentration was reduced from 10 % to 5 % (Miyamoto et al., 2012). We used iPSCs that had been previously cryopreserved in CryoStor® CS10, so it cannot be excluded that this had imposed a selective pressure on those iPSCs that selected out a nonrepresentative, DMSO freeze-resistant subpopulation.

This manuscript is fully relevant to the growing demand for robust cryopreservation methods with reduced DMSO content. Even low concentrations of DMSO have been demonstrated to alter cellular processes by modifying DNA methylation profiles, impacting gene expression, deregulating miRNAs as well as inducing differentiation (Erol et al., 2021). Cryopreservation studies of iPSCs have addressed issues such as aggregates vs single cell freezing, slow freezing vs vitrification, absence vs presence of small molecules such as ROCK inhibitor, and development of animal-component free cryosolutions. Few studies have been undertaken to test the cryopreservation of pluripotent stem cells using cryosolutions with less or no DMSO (Weng and Beauchesne, 2020). A controlled rate freezing study using DMSO-free trehalose-based cryosolutions containing ethylene glycol or glycerol achieved cryopreservation of iPSCs that the authors described as “acceptable” compared to the 10 % DMSO standard (Ntai et al., 2018). In our study, we demonstrate the fitness-for-purpose of 15 mM IRI in 5 % DMSO as an efficient cryoprotective solution for iPSCs in terms of their post-thaw recovery, viability, pluripotency, and transcriptomic changes. IRIs can reduce DMSO concentrations, thereby improving the utility, effectiveness, and efficiency of cryopreservation.

Credit authorship contribution statement

Kathleen Mommaerts: Formal analysis, Investigation, Methodology, Project administration, Visualization, Writing – original draft, Writing – review & editing. **Satoshi Okawa:** Data curation, Methodology, Software, Writing – review & editing. **Margaux Schmitt:** Methodology. **Olga Kofanova:** Methodology. **Tracey R. Turner:** Methodology, Resources. **Robert N. Ben:** Formal analysis, Methodology, Resources, Writing – review & editing. **Antonio Del Sol:** Data curation, Software, Supervision. **William Mathieson:** Formal analysis, Supervision, Writing – review & editing. **Jens C. Schwamborn:** Methodology, Supervision, Validation, Writing – review & editing. **Jason P. Acker:** Conceptualization, Formal analysis, Investigation, Methodology, Resources, Supervision, Validation, Writing – review & editing. **Fay Betsou:** Conceptualization, Formal analysis, Funding acquisition, Investigation, Methodology, Project administration, Resources, Supervision, Validation, Writing – review & editing.

Declaration of competing interest

The authors declare the following financial interests/personal relationships which may be considered as potential competing interests: Tracey R. Turner reports a relationship with PanTHERA CryoSolutions Inc. that includes: employment. Robert N. Ben reports a relationship with PanTHERA CryoSolutions Inc. that includes: board membership and employment. Jason P. Acker reports a relationship with PanTHERA CryoSolutions Inc. that includes: board membership and employment. Robert N. Ben has patent #US 9,648,869 B2 issued to University of Ottawa.

Acknowledgments

We thank Johanna Trouet, Camille Bellora, and Pauline Lambert for the help provided during the cryopreservation of the iPSCs. We thank the Luxembourg Parkinson’s study and the CRB-CHU Amiens, Biobanque de Picardie (Biobanking Resources Impact Factor: BB-0033-00017) for providing the skin biopsies. We thank Arnaud Muller for bioinformatic clarifications.

Appendix A. Supplementary data

Supplementary data to this article can be found online at https://doi.org/10.1016/j.scr.2024.103583.

Data availability

The complete dataset used in this study is available here: https://doi.org/10.17881/fpn5-th91.

References

Alasmar, S., Huang, J., Chopra, K., Baumann, E., Aylsworth, A., Hewitt, M., Sandhu, J.K., Tauskela, J.S., Ben, R.N., Jezierski, A., 2023. Improved cryopreservation of human induced Pluripotent Stem Cell (iPSC) and iPSC-derived neurons using ice-recrystallization inhibitors. Stem cells (Dayton, Ohio) 41 (2023), 1006–1021.

Ali, M., Khan, S.Y., Vasanth, S., Ahmed, M.R., Chen, R., Na, C.H., Thomson, J.J., Qiu, C., Gottsch, J.D., Riazuddin, S.A., 2018. Generation and proteome profiling of PBMC-originated, iPSC-derived corneal endothelial cells. Invest. Ophthalmol. Vis. Sci. 59, 2437–2444.

Arriza, J.L., Kavanaugh, M.P., Fairman, W.A., Wu, Y.N., Murdoch, G.H., North, R.A., Amara, S.G., 1993. Cloning and expression of a human neutral amino acid transporter with structural similarity to the glutamate transporter gene family. J. Biol. Chem. 268, 15329–15332.

Awan, M., Buriak, I., Fleck, R., Fuller, B., Goltsev, A., Kerby, J., Lowdell, M., Mericka, P., Petrenko, A., Petrenko, Y., Rogulska, O., Stolzing, A., Stacey, G.N., 2020. Dimethyl sulfoxide: a central player since the dawn of cryobiology, is efficacy balanced by toxicity? Regen. Med. 15, 1463–1491.

Babula, P., Masarik, M., Adam, V., Eckschlager, T., Stiborova, M., Trnkova, L., Skutkova, H., Provaznik, I., Hubalek, J., Kizek, R., 2012. Mammalian metallothioneins: properties and functions. Metallomics 4, 739–750.

Baust, J.M., Van, B., Baust, J.G., 2000. Cell viability improves following inhibition of cryopreservation-induced apoptosis, In vitro cellular & developmental biology. Animal 36, 262–270.

Baust, J.M., Vogel, M.J., Van Buskirk, R., Baust, J.G., 2001. A molecular basis of cryopreservation failure and its modulation to improve cell survival. Cell Transplant 10, 561–571.

Baust, J.M., Van Buskirk, R., Baust, J.G., 2002. Gene activation of the apoptotic caspase cascade following cryogenic storage. Cell Preservation Technology 1, 63–80.

Beere, H.M., Wolf, B.B., Cain, K., Mosser, D.D., Mahboubi, A., Kuwana, T., Tailor, P., Morimoto, R.I., Cohen, G.M., Green, D.R., 2000. Heat-shock protein 70 inhibits apoptosis by preventing recruitment of procaspase-9 to the Apaf-1 apoptosome. Nat. Cell Biol. 2, 469–475.

Briard, J.G., Jahan, S., Chandran, P., Allan, D., Pineault, N., Ben, R.N., 2016. Small-molecule ice recrystallization inhibitors improve the post-thaw function of hematopoietic stem and progenitor cells. ACS Omega 1, 1010–1018.

Chambers, S.M., Fasano, C.A., Papapetrou, E.P., Tomishima, M., Sadelain, M., Studer, L., 2009. Highly efficient neural conversion of human ES and iPS cells by dual inhibition of SMAD signaling. Nat. Biotechnol. 27, 275–280.

Chantelle, J.C., Malay, D., Robert, N.B., 2013. Ice recrystallization inhibitors: From biological antifreezes to small molecules, in: W. Peter (Ed.) Recent Developments in the Study of Recrystallization, IntechOpen, Rijeka, pp. Ch. 7
Chirikian, O., Feinstein, S.D., Faynus, M.A., Kim, A.A., Lane, K.V., Torres, G.V., Pham, J. V., Singh, Z., Nguyen, A., Thomas, D., Clegg, D.O., Wu, J.C., Pruitt, B.L., 2022. The effects of xeno-free cryopreservation on the contractile properties of human iPSC derived cardiomyocytes. J. Mol Cell Cardiol. 168, 107–114.
Crook, J.M., Tomaskovic-Crook, E., Ludwig, T.E., 2017. Cryobanking pluripotent stem cells. Methods in Molecular Biology (Clifton N.J.) 1590, 151–164.
D'Amour, K.A., Agulnick, A.D., Eliazer, S., Kelly, O.G., Kroon, E., Baetge, E.E., 2005. Efficient differentiation of human embryonic stem cells to definitive endoderm. Nat. Biotechnol. 23, 1534–1541.
De Belly, H., Paluch, E.K., Chalut, K.J., 2022. Interplay between mechanics and signalling in regulating cell fate. Nat. Rev. Mol. Cell Biol. 23, 465–480.
Deller, R.C., Pessin, J.E., Vatish, M., Mitchell, D.A., Gibson, M.I., 2016. Enhanced non-vitreous cryopreservation of immortalized and primary cells by ice-growth inhibiting polymers. Biomater. Sci. 4, 1079–1084.
Dinkova-Kostova, A.T., Talalay, P., 2010. NAD(P)H:quinone acceptor oxidoreductase 1 (NQO1), a multifunctional antioxidant enzyme and exceptionally versatile cytoprotector. Arch. Biochem. Biophys. 501, 116–123.
Dobin, A., Davis, C.A., Schlesinger, F., Drenkow, J., Zaleski, C., Jha, S., Batut, P., Chaisson, M., Gingeras, T.R., 2013. STAR: ultrafast universal RNA-seq aligner. Bioinformatics 29, 15–21.
Erol, O.D., Pervin, B., Seker, M.E., Aerts-Kaya, F., 2021. Effects of storage media, supplements and cryopreservation methods on quality of stem cells. World J. Stem Cells 13, 1197–1214.
Heng, B.C., Ye, C.P., Liu, H., Toh, W.S., Rufaihah, A.J., Yang, Z., Bay, B.H., Ge, Z., Ouyang, H.W., Lee, E.H., Cao, T., 2006. Loss of viability during freeze-thaw of intact and adherent human embryonic stem cells with conventional slow-cooling protocols is predominantly due to apoptosis rather than cellular necrosis. J. Biomed. Sci. 13, 433–445.
Hirokawa, N., 1994. Microtubule organization and dynamics dependent on microtubule-associated proteins. Curr. Opin. Cell Biol. 6, 74–81.
Hunt, C.J., 2011. Cryopreservation of human stem cells for clinical application: a review. Transfus. Med. Hemother 38, 107–123.
Kaindl, J., Meiser, I., Majer, J., Sommer, A., Krach, F., Katsen-Globa, A., Winkler, J., Zimmermann, H., Neubauer, J.C., Winner, B., 2019. Zooming in on cryopreservation of hiPSCs and neural derivatives: a dual-center study using adherent vitrification. Stem Cells Transl. Med. 8, 247–259.
Katkov II, M.S., Kim, R., Bajpai, Y.S., Altman, M., Mercola, J.F., Loring, A.V., Terskikh, E. Y., Snyder, F., 2006. Levine, Cryopreservation by slow cooling with DMSO diminished production of Oct-4 pluripotency marker in human embryonic stem cells. Cryobiology 53, 194–205.
Li, X., Meng, G., Krawetz, R., Liu, S., Rancourt, D.E., 2008. The ROCK inhibitor Y-27632 enhances the survival rate of human embryonic stem cells following cryopreservation. Stem Cells Dev. 17, 1079–1085.
Li, R., Yu, G., Azarin, S.M., Hubel, A., 2018. Freezing responses in DMSO-based cryopreservation of human iPS cells: aggregates versus single cells. Tissue Eng. Part C, Methods 24, 289–299.
Love, M.I., Huber, W., Anders, S., 2014. Moderated estimation of fold change and dispersion for RNA-seq data with DESeq2. Genome Biol. 15, 550.
Lv, X., Chen, Q., Zhang, S., Gao, F., Liu, Q., 2022. CGRP: a new endogenous cell stemness maintenance molecule. Oxid. Med. Cell Longev. 2022, 4107433.
Martin-Ibañez, R., Unger, C., Strömberg, A., Baker, D., Canals, J.M., Hovatta, O., 2008. Novel cryopreservation method for dissociated human embryonic stem cells in the presence of a ROCK inhibitor. Hum. Reprod. 23, 2744–2754.
Mathews, M., Wißfeld, J., Flitsch, L.J., Shahraz, A., Semkova, V., Breitkreuz, Y., Neumann, H., Brüstle, O., 2023. Reenacting neuroectodermal exposure of hematopoietic progenitors enables scalable production of cryopreservable iPSC-derived human microglia. Stem Cell Rev. Rep. 19, 455–474.
Miyamoto, Y., Noguchi, H., Yukawa, H., Oishi, K., Matsushita, K., Iwata, H., Hayashi, S., 2012. Cryopreservation of induced pluripotent stem cells. Cell Med. 3, 89–95.
Mommaerts, K., Bellora, C., Lambert, P., Türkmen, S., Schwamborn, J.C., Betsou, F., 2022. Method optimization of skin biopsy-derived fibroblast culture for reprogramming into induced pluripotent stem cells. Biopreserv. Biobanking 20, 12–23.
Monge, M., Colas, E., Doll, A., Gil-Moreno, A., Castellvi, J., Diaz, B., Gonzalez, M., Lopez-Lopez, R., Xercavins, J., Carreras, R., Alameda, F., Canals, F., Gabrielli, F., Reventos, J., Abal, M., 2009. Proteomic approach to ETV5 during endometrial carcinoma invasion reveals a link to oxidative stress. Carcinogenesis 30, 1288–1297.
Narumiya, S., Ishizaki, T., Uehata, M., 2000. Use and properties of ROCK-specific inhibitor Y-27632. Methods Enzymol. 325, 273–284.
Neaverson, A., Andersson, M.H.L., Arshad, O.A., Foulser, L., Goodwin-Trotman, M., Hunter, A., Newman, B., Patel, M., Roth, C., Thwaites, T., Kilpinen, H., Hurles, M.E., Day, A., Gerety, S.S., 2022. Differentiation of human induced pluripotent stem cells into cortical neural stem cells. Front. Cell Dev. Biol. 10, 1023340.
Ntai, A., La Spada, A., De Blasio, P., Biunno, I., 2018. Trehalose to cryopreserve human pluripotent stem cells. Stem Cell Res. 31, 102–112.
Poisson, J.S., Acker, J.P., Briard, J.G., Meyer, J.E., Ben, R.N., 2019. Modulating intracellular ice growth with cell-permeating small-molecule ice recrystallization inhibitors. Langmuir 35, 7452–7458.
Russell, F.A., King, R., Smillie, S.J., Kodji, X., Brain, S.D., 2014. Calcitonin gene-related peptide: physiology and pathophysiology. Physiol. Rev. 94, 1099–1142.
Sa, S., McCloskey, K., 2012. Activin A and BMP4 signaling for efficient cardiac differentiation of H7 and H9 human embryonic stem cells. Journal of Stem Cells & Regenerative Medicine 8, 198–202.
Shi, Z., Wei, Z., Li, J., Yuan, S., Pan, B., Cao, F., Zhou, H., Zhang, Y., Wang, Y., Sun, S., Kong, X., Feng, S., 2018. Identification and verification of candidate genes regulating neural stem cells behavior under hypoxia. Cell Physiol. Biochem. 47, 212–222.
Stossel, T.P., Condeelis, J., Cooley, L., Hartwig, J.H., Noegel, A., Schleicher, M., Shapiro, S.S., 2001. Filamins as integrators of cell mechanics and signalling. Nat. Rev. Mol. Cell Biol. 2, 138–145.
Subramanian, A., Tamayo, P., Mootha, V.K., Mukherjee, S., Ebert, B.L., Gillette, M.A., Paulovich, A., Pomeroy, S.L., Golub, T.R., Lander, E.S., Mesirov, J.P., 2005. Gene set enrichment analysis: a knowledge-based approach for interpreting genome-wide expression profiles. Proc. Natl. Acad. Sci. 102, 15545–15550.
Sugimoto, M.A., Vago, J.P., Teixeira, M.M., Sousa, L.P., 2016. Annexin A1 and the resolution of inflammation: modulation of neutrophil recruitment, apoptosis, and clearance. J. Immunol. Res. 2016, 8239258.
Takahashi, K., Tanabe, K., Ohnuki, M., Narita, M., Ichisaka, T., Tomoda, K., Yamanaka, S., 2007. Induction of pluripotent stem cells from adult human fibroblasts by defined factors. Cell 131, 861–872.
Tsankov, A.M., Akopian, V., Pop, R., Chetty, S., Gifford, C.A., Daheron, L., Tsankova, N. M., Meissner, A., 2015. A qPCR ScoreCard quantifies the differentiation potential of human pluripotent stem cells. Nat. Biotechnol. 33, 1182–1192.
Uhrig, M., Ezquer, F., Ezquer, M., 2022. Improving cell recovery: Freezing and thawing optimization of induced pluripotent stem cells. Cells 11.
Vidalino, L., Doria, A., Quarta, S., Zen, M., Gatta, A., Pontisso, P., 2009. SERPINB3, apoptosis and autoimmunity. Autoimmun. Rev. 9, 108–112.
Wagh, V., Meganathan, K., Jagtap, S., Gaspar, J.A., Winkler, J., Spitkovsky, D., Hescheler, J., Sachinidis, A., 2011. Effects of cryopreservation on the transcriptome of human embryonic stem cells after thawing and culturing. Stem Cell Rev. Rep. 7, 506–517.
Watanabe, K., Ueno, M., Kamiya, D., Nishiyama, A., Matsumura, M., Wataya, T., Takahashi, J.B., Nishikawa, S., Nishikawa, S., Muguruma, K., Sasai, Y., 2007. A ROCK inhibitor permits survival of dissociated human embryonic stem cells. Nat. Biotechnol. 25, 681–686.
Weng, L.D., Beauchesne, P.R., 2020. Dimethyl sulfoxide-free cryopreservation for cell therapy: a review. Cryobiology 94, 9–17.
William, N., Acker, J.P., 2020. Cryoprotectant-dependent control of intracellular ice recrystallization in hepatocytes using small molecule carbohydrate derivatives. Cryobiology 97, 123–130.
Wolkers, W.F., Oldenhof, H., 2021. Principles underlying cryopreservation and freeze-drying of cells and tissues, in: W.F. Wolkers, H. Oldenhof (Eds.) Cryopreservation and Freeze-Drying Protocols, Springer US, New York, NY, pp. 3-25.
Wood, B., Padula, M.P., Marks, D.C., Johnson, L., 2021. Cryopreservation alters the immune characteristics of platelets. Transfusion 61, 3432–3442.
Xu, X., Cowley, S., Flaim, C.J., James, W., Seymour, L., Cui, Z., 2010. The roles of apoptotic pathways in the low recovery rate after cryopreservation of dissociated human embryonic stem cells. Biotechnol. Prog. 26, 827–837.
Xu, L., Wang, L., Wen, Z., Wu, L., Jiang, Y., Yang, L., Xiao, L., Xie, Y., Ma, M., Zhu, W., Ye, R., Liu, X., 2016. Caveolin-1 is a checkpoint regulator in hypoxia-induced astrocyte apoptosis via Ras/Raf/ERK pathway. Am. J. Physiol. Cell Physiol. 310, C903–C910.
Yoshida, T., Maulik, N., Ho, Y.S., Alam, J., Das, D.K., 2001. H(mox-1) constitutes an adaptive response to effect antioxidant cardioprotection: a study with transgenic mice heterozygous for targeted disruption of the Heme oxygenase-1 gene. Circulation 103, 1695–1701.